Reprinted with permission from the publisher.
In: J. Vac. Sci. Technol. A. 2000. Vol. 18, No. 4,
pp. 1385–1389.

Deceleration of silicon etch rate at high aspect ratios

J. Kiihamäki[a)]
VTT Electronics, FIN-02044 VTT, Finland

(Received 30 September 1999; accepted 7 February 2000)

The molecular-flow conductance of a high aspect ratio feature can limit the etching species arriving at the bottom of the feature and thus limit the etch rate. A simple conductance model can predict the etch rate of the time-domain multiplexed etch process with good results at moderate-aspect ratios (5–20) for trenches, but at very high aspect ratios (>20) the conductance model breaks down. Other mechanisms are needed to explain the deceleration of etch rate and almost complete etch stop. In this article the reasons for etch stop at the bottom of deep features are discussed. Measurement results of deep silicon etching are presented. Very deep holes and trenches were etched into silicon to study the effect of process parameters. At moderate aspect ratios the bottom of the hole is nearly flat and the sidewalls are vertical. At high aspect ratio the sidewalls start to bow and the feature bottom turns into a sharp spearhead. The shape of the feature can have an impact on the step coverage of the passivation layer deposition during the passivation step and on passivation removal during the etch step, leading to excessive sidewall etching and reduced etch rate at the feature bottom. The nonzero sidewall reaction probability and flow conductance of tapered tubes were studied by Monte Carlo simulation. The main reason for deceleration of etching seems to be the loss of etchant species due to sidewall reactions combined with feature closure by ion-limited passivation polymer etching. © *2000 American Vacuum Society.* [S0734-2101(00)07904-5]

I. INTRODUCTION

Time-domain multiplexed etching (Bosch process) has recently gained popularity in high aspect ratio silicon etching for microelectromechanical systems (MEMS). Fluorine-based inductively coupled plasmas (ICP) using the Bosch process[1] have been shown to achieve etch rates of 3–7 μm/min at room temperature.[2,3] The Bosch process involves both gas flow and bias power cycling. Etch directionality is achieved with a sidewall-protecting polymer layer, which is deposited during the C_4F_8 passivating cycle. Silicon etching proceeds during the SF_6 etch cycle. The passivation polymer is removed from horizontal surfaces by ion-enhanced etching, after which silicon is etched isotropically from exposed areas by free fluorine. Nearly vertical profiles ($90° \pm 2°$) with simple photoresist or silicon dioxide masks can be achieved. Extensive presentations on etch parameter influences for resist masked processes have recently been published by Ayón and co-workers.[4,5]

Despite the merits of the Bosch process, some serious drawbacks exist such as aspect ratio-dependent etch rate and notching at the insulating etch stop layer. The aspect ratio-dependent etching (ARDE) is a serious limitation in deep silicon etching: at high aspect ratios excessive etch-rate reduction occurs with longer etch times.

ARDE in plasma etching has been attributed to a wide range of physical mechanisms. An excellent review of this topic has been published by Gottscho, Jurgensen, and Vitkavage.[6] Coburn and Winters[7] have introduced a simple conductance model based on Knudsen transport of particles in etched trenches, where the molecular-flow conductance limits the etching species arriving at the bottom of the feature. They derived the following equation for the ratio of the etch rate at the bottom of the feature $R(A)$ to the etch rate at the top of the feature $R(0)$:

$$R(A)/R(0)=K/(K+S-KS), \tag{1}$$

where S is the reaction probability on the bottom surface and K the molecular-flow transmission probability for a given tube or trench. A is the aspect ratio: depth/diameter for a circular hole or depth/width for a long trench. It was shown previously[8] that a simple conductance model can be used to predict the etch rate of a time-domain multiplexed inductively coupled plasma etch process with good results, when applied to linewidths typical of MEMS at moderate-aspect ratios. However, at very high aspect ratios the conductance model does not predict the almost total etch stop. Other mechanisms are needed to explain this deceleration of the etch rate. At moderate-aspect ratios the bottom of the hole is nearly flat and the sidewalls are nearly vertical. At high-aspect ratio the sidewalls start to bow and the feature bottom turns into a sharp arrowhead, as depicted in Fig. 1. The reasons for etch stop at the bottom of deep features are discussed here.

In many high aspect ratio silicon-etch processes the sidewall angle is negative for high etch-rate processes and positive for lower etch-rate process. The shape of the feature can have an impact on the passivation layer deposition during the passivation step and on passivation removal during the etch step, causing excessive sidewall etching and a reduced etch rate at the feature bottom. The shape also affects the molecular-flow conductance of a trench. A simple Monte Carlo simulation code was written to study the molecular-flow conductance in such tapered trenches. The simulation results of the effects of nonzero sidewall reaction probability

[a)]Electronic mail: Jyrki.Kiihamaki@vtt.

©2000 American Vacuum Society

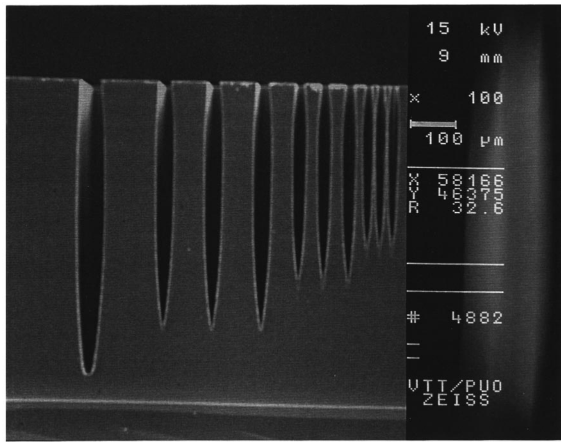

FIG. 1. Typical change in profile of etched trenches after 180 min etch time, nominal line widths 32, 16, 8, and 4 μm, minimum depth about 400 μm, and wafer thickness 1.3 mm.

and flow conductance of tapered tubes are presented here. The model with nonzero sidewall reaction coefficients is an intermediate case between the simple conductance model[7] and neutral shadowing discussed by Gottscho, Jurgensen, and Vitkavage.[6] The simulation program was also needed for generation of transport coefficients for arbitrary length rectangular trenches, because no practical values had been published or the maximum aspect ratios used in published work[9] were much smaller compared to aspect ratios achievable by etching. The high aspect ratio trenches with relatively vertical sidewalls obtained with the Bosch process form an almost ideal platform for simulation studies of reactant transport issues. In addition to the benefits of the etch profile, the relatively simple plasma with only one input gas at a time makes the isolation of different effects easier than traditional reactive ion etching reactors, where multiple input gases and simultaneous etching and deposition reaction occur. In studies of the Bosch process it is possible to decouple etching variables from passivation variables.[4]

Very deep holes were etched into silicon to study the effect of etch time and selected process parameters. The modeling results will be compared with new deep etch results.

II. EXPERIMENT

A. Processing of samples and measurement methods

Samples were processed on 100- and 150-mm-diam highly doped p-type silicon (0.02 Ω cm) wafers of ⟨100⟩ orientation. Silicon dioxide was used for masking. A contact aligner was used for lithography. The photolithography masks used were specially designed for this purpose. Oxide masks [thermal SiO_2 or chemical vapor deposited (CVD)] were defined by either plasma (100 mm wafers) or wet etch using buffered hydrofluoric acid (BHF) (150 mm wafers). The deep silicon etching was done with an STS Multiplex ICP etcher using STS ASE recipes.[2,3] Sample processing was done at the VTT Electronics process facilities, where most of the equipment is designed for 100-mm-diam wafers. A summary of the sample fabrication is shown in Table I.

TABLE I. Summary of sample processing steps used for two different sample types.

	Standard	6 in.
Wafer size: (mm)	100	150
Thickness (μm)	525	600
Mask oxide	CVD	Thermal
Mask thickness	2 μm	2 μm
Mask etch	Plasma	BHF
Drawn hole sizes	5–50 μm	50–120 μm
Used silicon etch times	10–120 min	90–120 min
Etchable area	8% (6.3 cm^2)	6% (11.1 cm^2)

Cycling conditions for our base-line high-etch-rate process were as follows: 13 s of etching with SF_6 (bias power 10 W) followed by 7 s of an unbiased C_4F_8 passivation step. The SF_6 flow was 129 sccm and the C_4F_8 flow 85 sccm. A constant coil power of 600 W and constant throttle valve position angle of 66° were used in both steps in all experiments. The additional processes used either a decreased SF_6 flow of 100 sccm or an increased rf bias of 15 W during etching, other process variables were kept constant.

The mask patterns used are described in earlier work.[3,8] The etchable area was 8% for 100 mm wafers and 6% for 150 mm wafers. The data do not allow direct comparisons over a wide range of etch times and pattern sizes because of variations in etchable area and sample manufacture. The oxide mask variations were unavoidable due to limited processing capabilities for 150 mm wafers. The different oxides behave similarly as the etch mask and have negligible or no effect on silicon etch rate, but the oxide mask etching method has an effect on the final mask dimensions.

Etched depth, the deepest point in the center of the trench, and etch profiles were determined with a Zeiss DSM 960 scanning electron microscope (SEM) from sawn cross sections from the center parts of the wafer.

B. Monte Carlo simulation of neutral transport

As flow conductances were not available for shapes other than long slit-like tubes and holes, a short Monte Carlo simulation code was written in basic-like language. The calculation was done on a desktop PC. The etch-rate modeling was later done using a spreadsheet program. The sample size N was kept at 100 000 throughout, giving an accuracy of simulation of about 0.3%.

First, the flow conductance values for rectangular tubes were calculated. Next, the same code was modified for other geometries. Particle transport was calculated using a similar method as described in Ref. 10. The maximum depth of each particle is recorded, and the molecular-flow coefficients are calculated from the particle statistics.

1. Geometrical considerations

Trajectories were calculated in three dimensions. The maximum aspect ratio, which in this case is the same as the

tube length, was set at 40. In deep silicon etching the typical aspect ratios fall within this range. In the case of infinite trenches the computation can be accelerated if the three-dimensional angular distribution is replaced by its in-plane equivalent, as discussed elsewhere.[11] This was not done here.

2. Angular distributions

The angular distribution functions for θ are generated from the following equation:

$$\frac{\int_0^{\Theta}\sin(\theta)\pi 2W(\theta)\partial\theta}{\int_0^{\pi/2}\sin(\theta)\pi 2W(\theta)\partial\theta}=\mathrm{RND}, \tag{2}$$

where RND is a random number and the weight function $W(\Theta)$ is the distribution function.

Selection of the angular distribution of incoming particles (from the plasma) has a notable effect on transport probability. The current simulations were done with a cosine distribution as this has been used in the handbook formulas[9] and in an earlier work.[8]

3. Sidewall losses

Sidewall losses were implemented using a random number generator. After each collision a new random number was generated and compared with a threshold value. If the threshold value was exceeded, the particle was deleted. No other reactions on the sidewalls or effects on the total etch rate given by Eq. (1) are assumed; the transport coefficients are merely attenuated in proportion to the number of deleted particles.

4. Tube shape

The transport probability of a tapered tube or a conical nozzle is different depending on which end of tube is the entrance. The transport probability is higher the larger the exhaust opening. Simulation results for low aspect ratio conical nozzles with positive opening angles can be found elsewhere.[10] Here, a short simulation is done for a tapered high aspect ratio slit-like tube.

5. Ion transport considerations

The depths of the first flight of particles can be used to evaluate the probability of particles reaching the bottom in one direct flight. This can then be used to estimate ion-shadowing effects, if the used angular distribution for incoming particles is realistic and ion deflection is negligible. These data are collected in each case. If ion-reflection calculations such as those done by Arnold, Gray, and Sawin[11] are needed, the number of reflections should be limited or more complete particle histories collected.

III. SIMULATION RESULTS

As a quick con dence check, the transport simulation results with cosine distribution were compared with results from handbook formulas for infinitely long slit-like tubes

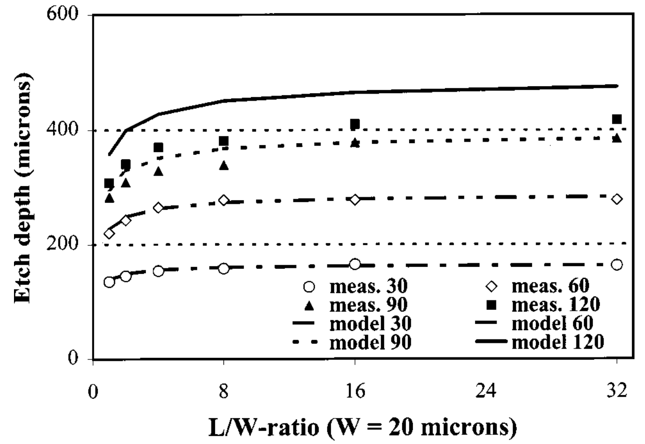

FIG. 2. Modeling results, nominal linewidth is 20 μm and etch times are 30, 60, 90, and 120 min.

and circular holes. The results were indistinguishable. An isotropic input distribution gives a much lower transport probability than a cosine distribution.

A. Rectangular patterns

After confirmation of simulation results for infinite trenches and holes, transport probabilities for rectangular trenches were calculated. The used length/width ratios are 1, 2, 4, 8, 16, and 32. When the length of the rectangular trench is 32 times the width, it can be considered an infinite length for most practical purposes. Squares and circular holes have small differences, the most notable difference occurs in lateral aspect ratios between one and two and between two and four. To ensure functionality of the etch-rate model, the new transport probabilities were inserted into the model and compared with the etching results. Model coefficients [$R(0)=7.27$ μm/min, $S=0.27$] and part of the etch data are from previous work;[8] the etch data from the 90 and 120 min etches are new and measured from 100-mm-diam wafers. A Comparison of the modeling results and measured data is shown in Fig. 2 and shows that the pattern shape dependency is modeled qualitatively correctly, but the depth of the samples with longer etch time is coarsely exaggerated.

B. Nonzero sidewall reaction probability

The effect of the sidewall reactions was calculated with reaction probabilities ranging from 0.0025 to 0.1 for both circular holes and infinite-length trenches. The lower limit is about 1% [of the observed apparent reaction probability at the bottom of the trenches. The modeled etch depths with transport probabilities of lossy tubes are shown in Fig. 3. The effect of losses is more pronounced for holes, which is understandable because the number of reflections required for particles reaching the bottom is larger. The effect of sidewall reactions can be notable, especially in the case of a low-reaction coefficient at the bottom, when the aspect ratio dependency is not expected, the sidewall losses can be the main cause of the aspect ratio dependency.

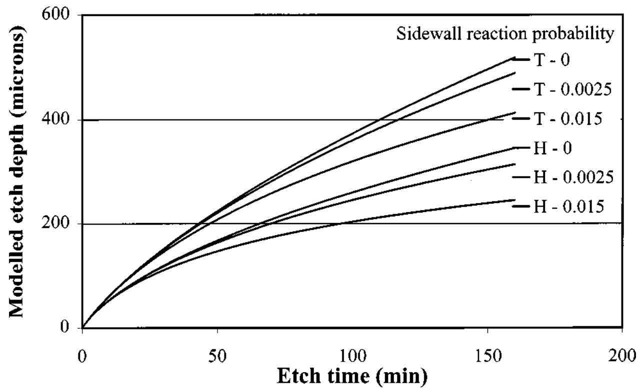

FIG. 3. Modeled etch depth as a function of time using transport probabilities of lossy trenches and holes with nominal linewidth of 20 μm, sidewall reaction probability as a parameter.

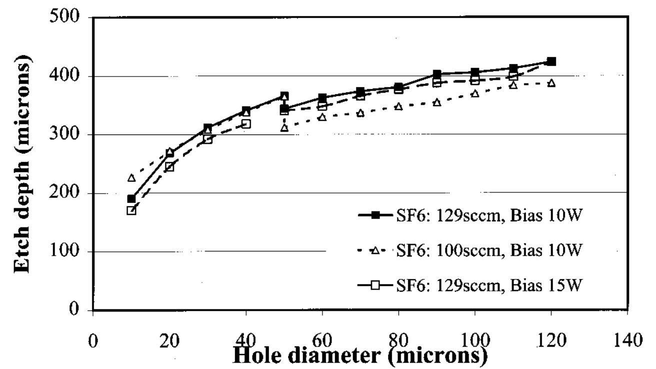

FIG. 5. Plot showing linewidth dependence of etch depth, SF_6 ow, and bias power as parameters.

C. Effect of nonvertical sidewalls

The effect of tilted sidewalls on reactant transport was calculated. As expected, the transport probability for negatively tapered profiles was notably higher than for tubes with a positive sidewall angle. However, the effect diminishes if the transport probability is scaled with the feature width at the given depth.

For a large negative sidewall angle, the total flux to the trench bottom may rise but the flux per area unit remains roughly constant. The number of particles reaching the bottom by direct flight will increase, but only in relation to the initial angular distribution. Unidirectional ion bombardment can cause large ion shadowing on high-negative sidewall angles.

The reactant transport differences of tapered trenches cannot explain the etch-rate difference between the high-rate process that has a negative sidewall angle and lower-rate processes that have a positive one. The relative etch rate is determined by the aspect ratio only. The sidewall angle may have a more important role during the passivation step, as the deposited passivation-layer thickness may differ on differently oriented surfaces.

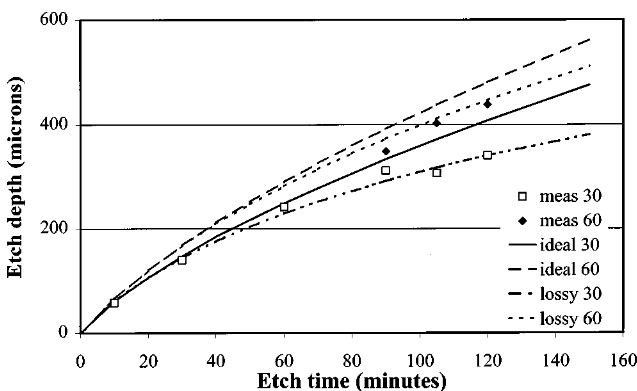

FIG. 4. Etch depths of 30- and 60-μm-diam holes as a function of etch time. The markers indicate measured data, the lines indicate the modeled data. Sidewall reaction coefficient of 0.015 is used in modeling of lossy circular tubes.

IV. MEASUREMENT RESULTS

The measurement results of 30- and 60-μm-diam holes are shown in Fig. 4. The modeling results are plotted in Fig. 4 together with the measured data. The total width of the nominally 60 μm oxide mask opening is about 69 μm after wet etching of the mask and 90 min of dry etching. For the dry-etched mask an average of 3.7 μm total widening was observed after 10–80 min silicon etching. In modeling, a 4 μm offset was used when defining the aspect ratio. The scatter in the lower measured data curve is partly caused by positional inaccuracy of SEM cross sectioning.

The etch depth of circular holes as a function of hole diameter is plotted in Fig. 5. The discontinuity in curves is caused by the loading effect.

The SF_6 flow and bias power are used as parameters. The Etch time is 90 min. As Fig. 5 shows, the etch rate is slightly higher for the smallest features with the lowered SF_6 flow than with our standard process. For larger holes the standard process is faster. The shape of the bottom of the features is flatter for the case of lower SF_6 flow. The latter is true for the case of higher bias power, too.

V. DISCUSSION

Reactant transport has a major effect on the etch rate of high aspect ratio features. The modeling results of this (Fig. 2) and previous work[8] confirm that a molecular-flow conductance model can predict the etch depth correctly for a wide range of shapes. However, for the highest-aspect ratios the model gives overly optimistic etch depths. Possibly this can be attributed to losses due to sidewall reactions. At higher-aspect ratios the ion flux can deteriorate the thin sidewall passivation layer, thus making sidewalls prone to etching. Also, the surface roughness increases during etching, which can make the sidewalls even more vulnerable. In Fig. 4 the etch depths are modeled for both lossless and lossy cases. In the lossy model the sidewall reaction coefficient is set to 0.015. Using this reaction coefficient together with the earlier model parameters gives an improved fit for 60-μm-diam holes compared to lossless transport. The sidewall reaction coefficient value 0.015 may give too low a value for etch depth, because the actual depths of 30 μm holes can be

higher compared to the measured values due to positioning inaccuracy and that the 60 μm hole data are from samples with higher pattern loading. However, the trend of the etch-rate deceleration compared to the ideal case is clear and is seen also in Fig. 2.

In high-density plasmas the number of ionized particles is considerably higher than in the plasmas used in traditional reactive ion etching. Comparison of the observed high reaction probabilities (in the range 0.2–0.3) with the reaction probability data of Gray, Tepermeister, and Sawin[12] suggests that the neutral-flux-to-ion-flux ratio is very low and that the silicon etching is neutral limited.

In addition to sidewall etching, the feature bottom changes from flat-bottom sharp-edged feature to rounded-bottom corners and eventually features close up. This can be a factor causing the scatter of the measurement data of 30 μm holes of Fig. 4. In practice, the complete clearing of the trench is usually required and then a further extension in etch time is needed.

This kind of feature evolution does not arise from neutral diffusion. The most likely reason for this profile change is the deficient or slowed-down passivation polymer removal during the etch step. At high aspect ratios the ion shadowing limits the polymer etching. So the overall etch process is no longer purely neutral limited, becoming instead ion limited as the aspect ratio increases. For circular holes the critical-aspect ratio is in the range of 10:1. This figure is obtained from feature profile inspection. In earlier measurements,[8] the highest-aspect ratios obtained for trenches were about 35:1 and the critical-aspect ratio is below this for the etch process used in these studies. Determination of the critical-aspect ratio of long trenches would require more measured data on extremely deep-etched trenches or knowledge on the width of the incoming ion angular distribution. An approximation of neutral flux as a function of the aspect ratio can be obtained from the molecular-flow model.

If the incident ion flux limits the passivation removal, then a higher or more directed ion flux is needed at the beginning of the etch step. For profile control it would be ideal to keep the etching in the neutral-limited regime all the time. However, the increase of ion directivity by either increasing bias or lowering the pressure will lower the etch selectivity against the masking material. Parameter ramping schemes where, among other parameters, platen (bias) power is increased during etching to ensure profile control, while the aspect ratio is changing continuously, have been recently developed by at least one equipment manufacturer.[13,14] The simple modeling strategy used in this article may not be applicable in the case of parameter ramping where the $R(0)$ is continuously changed during the etching.

The high reaction probabilities obtained with a simple, lossless etch model may already include the effect of transport losses due to sidewall reactions. Similar modeling results may be obtained with a model utilizing low bottom-reaction probability and high sidewall-reaction probabilities. To ensure the quality of the model, realistic reaction probabilities are needed, which is probably a difficult task in the case of sidewall reactions, as the thickness of the sidewall protecting layer can be indeterminate and the reaction probabilities can vary with depth.

The tube shape can also have an impact on reactant transport. The Monte Carlo simulation shows that the tapered tube has an effect on tube directivity.[10] In the case of bowed profiles it is possible that the molecules are trapped in the middle parts of the tube, where it is widest, and cause further bowing.

Utilization of Gaussian or other applicable distributions to evaluate ion transport into trenches is planned in future studies. The most serious obstacle in improving the etch-rate model is the lack of information on aspect ratio dependency of passivation polymer deposition and etching.

VI. CONCLUSIONS

The molecular-flow conductance model is used to predict the etch depth of trenches of various shapes. The aspect ratio dependency of the etch rate of the Bosch process is explained reasonably both qualitatively and quantitatively by molecular-flow conductance. It is shown with the help of Monte Carlo simulation that sidewall reactions can have a notable effect on etch rate as the aspect ratio increases. At higher aspect ratios the passivation polymer etching becomes ion-flux limited, while silicon etching remains in the neutral-limited regime. The measurement results indicate that higher-aspect ratios can be achieved with increased ion directionality and the amount of lateral etching can be decreased at the same time.

ACKNOWLEDGMENTS

This work was funded by VTT Electronics, TEKES (The National Technology Agency, Finland) and VTI Hamlin. Many thanks to Sami Franssila and Jani Karttunen for their help with the sample preparation and reviewing of the manuscript.

[1] F. Lärmer and A. Schilp, German Patent No. DE4241045.
[2] J. K. Bhardwaj and H. Ashraf, Proc. SPIE **2639**, 224 (1995).
[3] J. Kiihamäki and S. Franssila, Phys. Scr. **T79**, 250 (1999).
[4] A. A. Ayón, R. Braff, C. C. Lin, H. H. Sawin, and M. A. Schmidt, J. Electrochem. Soc. **146**, 339 (1999).
[5] A. A. Ayón, R. A. Braff, R. Bayt, H. H. Sawin, and M. A. Schmidt, J. Electrochem. Soc. **146**, 2730 (1999).
[6] R. A. Gottscho, C. W. Jurgensen, and D. J. Vitkavage, J. Vac. Sci. Technol. B **10**, 2133 (1992).
[7] J. W. Coburn and H. F. Winters, Appl. Phys. Lett. **55**, 2730 (1989).
[8] J. Kiihamäki and S. Franssila, J. Vac. Sci. Technol. A **17**, 2280 (1999).
[9] J. F. O'Hanlon, *A User's Guide to Vacuum Technology*, 2nd ed. (Wiley, New York, 1989), pp. 438–439.
[10] D. H. Davis, L. L. Levenson, and N. Milleron, in *Rare ed Gas Dynamics*, edited by L. Talbot, (Academic, New York, 1961), p. 99.
[11] J. C. Arnold, D. C. Gray, and H. H. Sawin, J. Vac. Sci. Technol. B **11**, 2071 (1993).
[12] D. C. Gray, I. Tepermeister, and H. H. Sawin, J. Vac. Sci. Technol. B **11**, 1243 (1993).
[13] J. Hopkins, H. Ashraf, J. K. Bhardwaj, A. M. Hynes, I. Johnston, and J. N. Shepherd, Mater. Res. Soc. Symp. Proc. **546**, 63 (1999).
[14] A. M. Hynes, H. Ashraf, J. K. Bhardwaj, J. Hopkins, I. Johnston, and J. N. Shepherd, Sens. Actuators A **74**, 13 (1999).